 DOI: 10.1002/masy.200651324

Three-Dimensional Observations of Grain Boundary Morphologies in a Cylinder-Forming Block Copolymer

Hiroshi Jinnai,[*1] *Kaoru Yasuda,*[1] *Toshio Nishi*[2]

Summary: The grain boundary morphology of a cylinder-forming poly(styrene*block*-isoprene) (SI) diblock copolymer was investigated using transmission electron microtomography (TEMT). The three-dimensional (3D) morphologies of the grain boundaries between the two grains with different orientation angle, α, were investigated. In the present study, two kinds of grain boundary morphologies, $\alpha \simeq 90^\circ$ and $\alpha \simeq 120^\circ$, were examined in 3D. It was found that, in the case of $\alpha \simeq 90^\circ$, most of the cylindrical domains bent at the grain boundary in order not to intersect each other, while the cylindrical domains were found to be smoothly connected and were continuous in the case of $\alpha \simeq 120^\circ$. The observed morphologies indicated that the chain conformation inside the cylindrical microdomains plays more significant role than the segmental interaction between the two blocks.

Keywords: block copolymers; cylindrical structure; microphase-separated structure; three-dimensional reconstruction; transmission electron microtomography

Introduction

Block copolymers often exhibit nanodomain structures with various morphologies.[1,2] The macroscopic properties of such systems depend not only on the local structure in the mesoscopic scale of $10 \sim 100$ nm but also on the long-range order on a scale of micrometers or larger. The three-dimensional (3D) morphology between grain boundary regions influences the mechanical, electrical, and diffusional properties[3,4] of block copolymer. Although important, the 3D continuity of each nanodomain at the grain boundary is not trivial.

The grain boundary morphologies in lamellar structure of block copolymers have been a subject for more than a decade.[5–10] The grain boundaries in the lamella-forming block copolymers can be divided into two types: the kink (tilt) grain boundary (KGB) and the twist grain boundary (TGB). In the KGB, normals to the lamellae of two neighboring grains establish a plane that is perpendicular to the boundary surface. In the TGB, on the other hand, the plane is parallel to the boundary surface. The KGB of block copolymers has been intensively studied, both experimentally[6,8–10] and theoretically.[11] Thomas *et al.* proposed the doubly periodic morphology approximating Scherk's first surface as a model for the TGB simply due to the minimization of the surface area,[12] which was later confirmed experimentally by *Jinnai et al.*[13] In contrast to the KGB, there are only a few experimental studies concerning the structure of TGBs in the literature[6,7] and, to our best knowledge, there are no study dealing with the grain boundaries in the cylinder-forming block copolymers.

The fact that the number of the experimental studies are somehow limited until

[1] Department of Macromolecular Science and Engineering, Kyoto Institute of Technology, Matsugasaki, Kyoto 606-8585, Japan
Fax: +81-75-724-7770
E-mail: hjinnai@kit.ac.jp
[2] Department of Organic and Polymeric Materials, School of Science and Engineering, Tokyo Institute of Technology, 2-12-1, Ohokayama, Meguro-ku, Tokyo 152-8552, Japan

now is partly due to the lack of appropriate experimental techniques for 3D real-space volume imaging. Although transmission electron microscopy (TEM) provides real-space images of the grain boundary structures, they are not always conclusive because (i) they are two-dimensional (2D) projections of 3D morphologies and (ii) the orientation of the grain boundary in the ultrathin section varies indefinitely, giving rise to a variety of patterns. Therefore, it would be preferable to *directly* observe the grain boundary structures.

Transmission electron microtomography (TEMT) allows one to obtain a 3D image of the structural object[14] and, after an appropriate image analysis, to evaluate its structural parameters.[15] Block copolymer microphase-separated structures have been studied in 3D by TEMT,[16–20] some of which quantitatively characterized complex morphologies to evaluate their structural parameters from 3D digital data.[18,19] Recently, an improved and more advanced 3D visualization technique, e.g., dual-axis electron tomography[21] and ''perfect'' electron tomography,[22] for anisotropic nanostructures, e.g., cylinders, have been developed. In the present study, we take full advantage of the TEMT to study the grain boundary morphologies of a cylinder-forming block copolymer.

Experimental Part

Materials

Poly(styrene-*block*-isoprene) (SI) was purchased from Polymer Source, Inc., Canada. The number-average molecular weight (M_n) of the PS and PI blocks was 40,800 and 10,400, respectively. The volume fraction of PI in the SI copolymer was 0.23. The polydispersity index (PDI), M_w/M_n, for the diblock copolymer was 1.06. The molecular weight and PDI were determined by size exclusion chromatography. The block copolymer composition was calculated from the ^{1}H-NMR spectra by comparing the peak area of the vinyic isoprene proton with the aromatic protons of polystyrene.

A. Specimens

A film specimen was prepared by casting from a ca. 5 wt% toluene solution. The cast film was annealed at 140 °C for 24 h under vacuum, which was subsequently stained by exposing the film to osmium tetraoxide (OsO_4) vapor for 1 day. The obtained stained film was ultramicrotomed with a diamond knife at room temperature using a Lica Ultracut UCT. The ultrathin section was transferred onto a Cu mesh grid with a polyvinylformal substrate. Prior to the TEMT observations, 5 nm Au nanoparticles (GCN005, BBInternational, Ltd., UK) were deposited from an aqueous suspension and then coated with a thin layer of evaporated carbon to promote specimen stability under the electron beam.

B. Transmission Electron Microtomography (TEMT)

TEMT experiments were performed using an energy-filtering transmission electron microscope with a field-emission gun operated at 200 kV (JEM-2200FS, JEOL Co., Ltd., Japan). Projections were collected with a slow-scan CCD camera (Gatan USC1000, Gatan, Inc.). Note that only the transmitted and elastically scattered electrons (electron energy loss of 0 ± 15 eV) were selected by an in-column energy filter installed in the JEM-2200FS (Omega filter, JEOL, Ltd., Japan) in order to obtain achromatic projections. Note that the optical axis of the microscope is z-axis throughout this paper. A series of TEM images were acquired at tilt angles ranging from $-60°$ to $+60°$ at the angular interval of $1°$. Subsequently, the tilt series of the TEM images (121 images) were aligned and reconstructed to generate 3D images according to the same protocol described earlier.[13,15,19]

Results and Discussion

Figure 1 shows TEM micrographs of SI triblock copolymer observed in two different fields of view. In Figure 1(a), most of the cylinders were in the x-y plane, but their

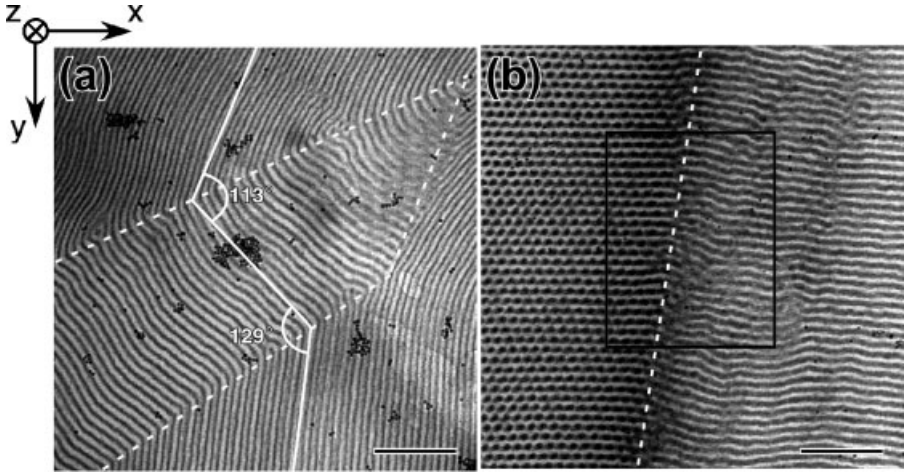

Figure 1.
TEM micrographs of grain boundary morphologies: (a) $\alpha \simeq 120^\circ$ and (b) $\alpha \simeq 90^\circ$. SI block copolymer was stained by OsO_4. Gray domains are PI microdomains. Dashed and solid lines represent, respectively, the grain boundaries and the orientation of the cylinders. Small dots in the micrographs are Au nano-particles that were used for aligning the tilt series in the TEMT experiments. A rectangle in part (b) shows the area where the TEMT experiment were carried out. Bar represents 200 nm.

orientations varied at the grain boundaries. The orientation angle, α, between the upper and lower boundaries (shown by the dashed lines) appeared to be 113° and 129°, respectively. On the other hand, in Figure 1(a), the hexagonally-packed cylindrical microdomains in left side of the picture were edge-on geometry, i.e., parallel to the z-axis and the cylinders in the right grain were horizontally aligned. Thus, $\alpha \simeq 90^\circ$. The two grains collided to form the grain boundary region in the middle of the TEM picture (indicated also by the white dashed line).

The TEMT experiments was carried out in the two fields of view to observe their 3D morphologies. Figure 2(a) displays 3D reconstructed image of the grain boundary with $\alpha \simeq 120^\circ$, which is the same field of view shown in Figure 1(a). Several cylindrical microdomains were chosen and displayed in Figure 2(b) in order to demonstrate the continuity of the microdomains across the grain boundary. The cylinders marked by 'A' were continuous through the three grains. In the grain boundary region marked by 'B', however, two cylinders were merged at the upper grain boundary and the resulting single cylinder went downwards at the lower grain boundary. In addition, as shown in the region marked by 'C', some cylindrical microdomains were disconnected at the grain boundary. Such link-up and discontinuity of the cylindrical microdomains across the grain boundary is due to the mismatch of hexagonal lattice of the cylinders across the grain boundary. Nonetheless, in general, the majority of the cylindrical microdomains were continuous and changed their directions between the grains.

Figure 3(a) shows 3D reconstructed image of the grain boundary with $\alpha \simeq 90^\circ$. Note that the 3D image corresponds to the rectangular area in Figure 1(b). The cylindrical microdomains were vertically and horizontally aligned in the left and right sides of the 3D reconstruction, respectively. The grain boundary lay between the two regions. In order to clarify the grain boundary morphology in such a geometry, some of the cylindrical microdomains in the right grain were displayed in the same manner as in Figure 2(b). It is quite intriguing that the cylinders bent downwards and did not collide against vertical

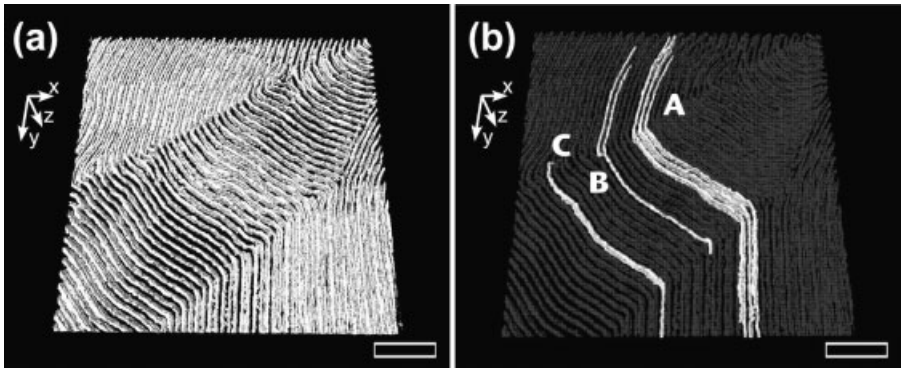

Figure 2.
(a) 3D reconstructed image of grain boundary morphology corresponding to TEM micrograph shown in Figure 1(a). Some of the cylinders were highlighted in part (b) in order to show connectivity (and discontinuity) of the cylinders across the boundary. Bar represents 200 nm.

cylinders in the left. As a matter of fact, all the horizontal cylinders in Figure 3(a) just bent (or disconnected at the edge of the grain), and did not run into the vertical cylinders: The cylindrical microdomains were rarely combined at the grain boundary. Figure 3(c) shows such rare example where the horizontal cylinders collide with the vertical ones. Note that the 3D reconstructed image in Figure 3(c) was taken in different field of view from that shown in Figure 3(a).

In any case, it is very likely that the collision of the cylindrical microdomains across the grain boundaries was avoided. Figure 4 Schematically shows block copolymer chains in the two representative cylindrical microdomains found at the grain boundary. If the cylindrical microdomains intersect at the boundary as shown in Figure 4(a), the blocks consisting of matrix, i.e., polystyrene (PS) in this case, may heavily overlap around the junction, forcing PS blocks to collapse in order to realize uniform segmental density distribution in the system. The entropic penalty due to the contraction of the block copolymer chains increases the total free energy of the system. On the contrary, if the cylindrical microdomains bend at the grain boundary as shown in Figure 4(b), the block copolymers can be accommodated without paying as much entropic penalty as in the previous case. Thus, the chain conformation seems to control the grain boundary morphologies in the cylinder-forming block copolymers.

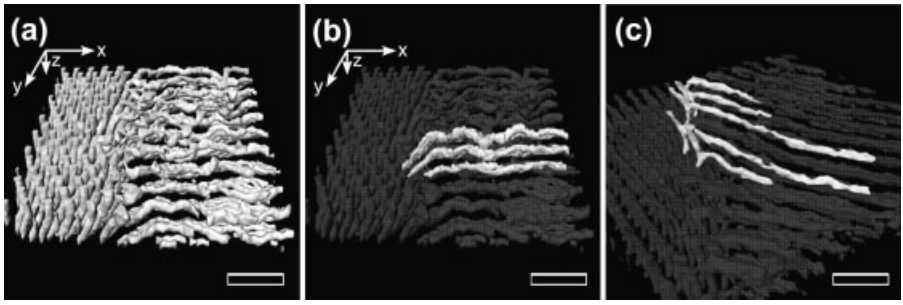

Figure 3.
(a) 3D reconstructed image of grain boundary morphology corresponding to TEM micrograph shown in Figure 1(b). The cylindrical microdomains in the left are edge-on, while those in the right are horizontally aligned. Some cylinders were highlighted in part (b). The intersecting cylinders found in different field of view from those in Figures 1(b) and 3(a) are shown in part (c). Bar represents 100 nm.

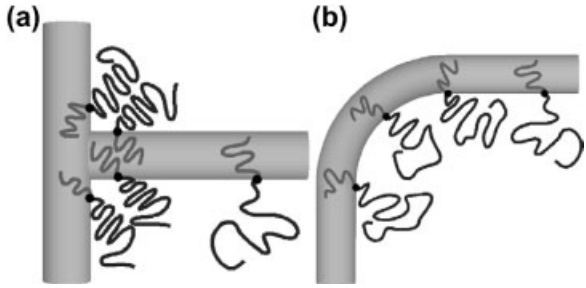

Figure 4.
Schematic illustration of block copolymer chains inside (a) intersecting cylinders and (b) bended cylinders.

Summary

The grain boundary morphology of a cylinder-forming poly(styrene-*block*-isoprene) (SI) diblock copolymer was studied using transmission electron microtomography (TEMT). The three-dimensional (3D) morphologies at the grain boundaries were visualized and the cylindrical microdomains in the vicinity of the boundaries were carefully traced. Two grain boundaries with $\alpha \simeq 90^\circ$ and $\alpha \simeq 120^\circ$ (α is the orientation angle between the cylinders) were examined. It was found, in both cases, that the cylinders tended to change their directions at the boundaries so that they avoided colliding with other cylinders. The block chain conformation, i.e. entropy, is the primary cause of such grain boundary morphologies, which is in sharp contrast to the lamellar-forming block copolymers case where the enthalpy between the two blocks plays a dominant role in the formation of the grain boundary morphologies.[12,13]

Acknowledgements: The authors are grateful to NEDO for supporting this study through the Japanese National Project ''Nano Structured Polymer Project'' by the Ministry of Economy, Trade and Industry.

H. J. is grateful to the Ministry of Education, Science, Sports and Culture for support of this research through Grait-in-Aid No. 1855019.

[1] I. W. Hamley, *Nanotechnology* **2003**, *14*, R39.
[2] V. Abetz and P. F. W. Simon, *Adv. Polym. Sci.* **2005**, *189*, 125.
[3] D. Ehlich, M. Takenaka, S. Okamoto, and T. Hashimoto, *Macromolecules* **1993**, *26*, 189.
[4] D. Ehlich, M. Takenaka, and T. Hashimoto, *Macromolecules* **1993**, *26*, 492.
[5] Y. Nishikawa, H. Kawada, H. Hasegawa, and T. Hashimoto, *Acta Polym.* **1993**, *44*, 247.
[6] S. P. Gido, J. Gunther, E. L. Thomas, and D. Hoffman, *Macromolecules* **1993**, *26*, 4506.
[7] S. P. Gido and E. L. Thomas, *Macromolecules* **1994**, *27*, 849.
[8] L. Qiao and K. I. Winey, *Macromolecules* **2000**, *33*, 851.
[9] L. Qiao, K. I. Winey, and D. C. Morse, *Macromolecules* **2001**, *34*, 7858.
[10] L. Qiao, A. J. Ryan, and K. I. Winey, *Macromolecules* **2002**, *35*, 3596.
[11] M. W. Matsen, *J. Chem. Phys.* **1997**, *107*, 8110.
[12] E. L. Thomas, D. M. Anderson, C. S. Henkee, and D. Hoffman, *Nature (London)* **1988**, *334*, 598.
[13] H. Jinnai, K. Sawa, and T. Nishi, *Macromolecules* **2006**, *39*, 5815.
[14] J. Frank, Plenum Press, New York, **1992**.
[15] H. Jinnai, Y. Nishikawa, T. Ikehara, and T. Nishi, *Adv. in Polym. Sci.* **2004**, *170*, 115.
[16] R. J. Spontak, M. C. Williams, and D. A. Agard, *Polymer* **1988**, *29*, 387.
[17] L. H. Radzilowski, B. O. Carragher, and Si. I. Stupp, *Macromolecules* **1997**, *30*, 2110.
[18] H. Jinnai, Y. Nishikawa, R. J. Spontak, S. D. Smith, D. A. Agard, and T. Hashimoto, *Phys. Rev. Lett.* **2000**, *84*, 518.
[19] H. Nishioka, K. Niihara, T. Kaneko, Y. Nishikawa, J. Yamanaka, T. Inoue, T. Nishi, and H. Jinnai, *Compos. Interfac.* **2006**, *13*, 589.
[20] T. Kaneko, K. Suda, K. Satoh, M. Kamigaito, T. Kato, T. Ono, E. Nakamura, T. Nishi, and H. Jinnai, *Macromolecular Symposia*, in press.
[21] H. Sugimori, T. Nishi, and H. Jinnai, *Macromolecules* **2005**, *38*, 10226.
[22] N. Kawase, M. Kato, H. Nishioka, and H. Jinnai, *Ultramicroscopy*, in press.

